

Finite element modelling of winged suction caissons in clay under uniaxial and combined loading

Darby, Laurence; Faramarzi, Asaad; Faizi, Koohyar; Mehravar, Moura; Harireche, Ouahid

License:

None: All rights reserved

Document Version

Peer reviewed version

Citation for published version (Harvard):

Darby, L, Faramarzi, A, Faizi, K, Mehravar, M & Harireche, O 2019, 'Finite element modelling of winged suction caissons in clay under uniaxial and combined loading', Paper presented at 2nd International Conference on Natural Hazards and Infrastructure, Chania, Greece, 23/06/19 - 26/06/19.

[Link to publication on Research at Birmingham portal](#)

Publisher Rights Statement:

Checked for eligibility: 26/07/2019

General rights

Unless a licence is specified above, all rights (including copyright and moral rights) in this document are retained by the authors and/or the copyright holders. The express permission of the copyright holder must be obtained for any use of this material other than for purposes permitted by law.

- Users may freely distribute the URL that is used to identify this publication.
- Users may download and/or print one copy of the publication from the University of Birmingham research portal for the purpose of private study or non-commercial research.
- User may use extracts from the document in line with the concept of 'fair dealing' under the Copyright, Designs and Patents Act 1988 (?)
- Users may not further distribute the material nor use it for the purposes of commercial gain.

Where a licence is displayed above, please note the terms and conditions of the licence govern your use of this document.

When citing, please reference the published version.

Take down policy

While the University of Birmingham exercises care and attention in making items available there are rare occasions when an item has been uploaded in error or has been deemed to be commercially or otherwise sensitive.

If you believe that this is the case for this document, please contact UBIRA@lists.bham.ac.uk providing details and we will remove access to the work immediately and investigate.

Finite element modelling of winged suction caissons in clay under uniaxial and combined loading

L. W. Darby, A. Faramarzi, K. Faizi
University of Birmingham, UK

M. Mehravar¹
Aston University, UK

O. Harireche
Islamic University of Madina, KSA

ABSTRACT

Suction caisson foundations, also known as skirted foundations, have recently become a relatively popular solution to support offshore wind turbines. These foundations however, have limited capacity compared to monopiles, particularly when exposed to combined loads reflective of those imposed by offshore wind turbines. The situation may become worse with the introduction of hyper-tall wind turbines and the increasing intensity of storms, including the possibility of hurricanes, which will impose large torsional and overturning moments on the superstructure. This study proposes an innovative solution for foundations of offshore wind turbines in the form of a winged suction caisson which can enhance the torsional capacity of the foundation. In this research, finite element models of the proposed foundation are developed to study its performance in clay under torsional loading combined with horizontal and overturning loads. The results are presented graphically using failure envelopes. The results show a substantial improvement in the overall capacity of the foundation with the addition of wings under combined loading (at least over 40% increase) compared to a conventional suction caisson foundation.

Keywords: suction caisson foundation, offshore wind turbines, undrained, torsion, combined loading.

INTRODUCTION

The UK has the ambition to achieve 50 GW of offshore wind electricity by 2050 (*Department of Energy and Climate Change, 2011*). Similar goals have been set by other countries e.g. The United States require 404GW of electricity to be generated from wind by 2050. To achieve this target, 86GW of electricity will be provided by offshore wind turbines (OWT) situated in the Gulf of Mexico (*Rose et al, 2012; Department of Energy, 2016*). To date, the majority of OWT have been constructed in Europe, with 82% of them founded on monopile foundations, which account for approximately 20% of the overall project cost. There is a precedence in finding alternative low-cost solutions for foundation of offshore wind turbine.

One innovative solution is suction caisson foundation (SCF) which comprises an upturned bucket of steel, with the skirts of the foundation protruding into the seabed. This design can be up to 20% cheaper, both in terms of materials and installation cost, compared with conventional foundations e.g. monopile (*Knudsen and Ostergaard, 2013; Carrington, 2013*). In addition, the method of installation of the foundation is a lot simpler and quicker than for other types of foundation and it can be easily removed at the end of its design life, making it a more sustainable solution (*Byrne, 2000; Byrne et al, 2002*).

¹ Corresponding Author: Moura Mehravar, *Aston University, M.Mehravar@aston.ac.uk*

Thus far research into the capacity of the SCF has focused primarily on the interaction of vertical, horizontal and moment loading (Gourvenec, 2008; Hung and Kim, 2014). As OWT are relatively light in comparison to other structures it is considered that horizontal loads and moments are the key factors that will govern the design criterion (Kim et al, 2016; Mehravar et al, 2016). However, with the intensity of tropical storms and the demand to construct OWT in hurricane prone regions increasing, it is critical that the torsional capacity of the SCF is assessed (Emanuel, 2005). Torsional loads are transferred from the wind turbine into the foundation system due to large eccentric forces applied to the superstructure (Taiebat and Carter, 2005). Only a limited number of studies have assessed the torsional capacity of SCFs. Those that have considered torsional loading, have modelled suction caissons/piles acting as part of an anchor system subjected to eccentric horizontal loading due to misalignment of the pad eye (Taiebat and Carter, 2005; Suroor and Hossain, 2015). Taiebat and Carter (2005) found that for a single embedment to diameter ratio of two, the horizontal and vertical capacity of a suction pile is reduced with torsional loading. Consequently, if the effect of torsional loading is not considered then the capacity of the SCF will be overestimated. The need to consider torsional loading is of growing significance as the height of OWT are increasing annually, resulting in larger moments being transferred to the foundation (Department of Energy, 2016; Mawer and Kalumba, 2016). Therefore, to increase the capacity of SCFs various modifications have been proposed in recent years, which include the addition of a peripheral skirt or an internal honeycomb structure (Bienen et al., 2012; Li et al., 2015). It was concluded that these systems improve the moment and lateral capacity of the SCF. However, the torsional capacity of these modified SCFs was not considered so additional investigations are required before they can be utilized.

In this paper an innovative solution is proposed to enhance bearing capacity of SCFs. This new solution, involves the addition of ‘wings’ to SCF. Four wings are attached to the skirt in vertical positions at 90-degree intervals, as illustrated in Fig. 1a.

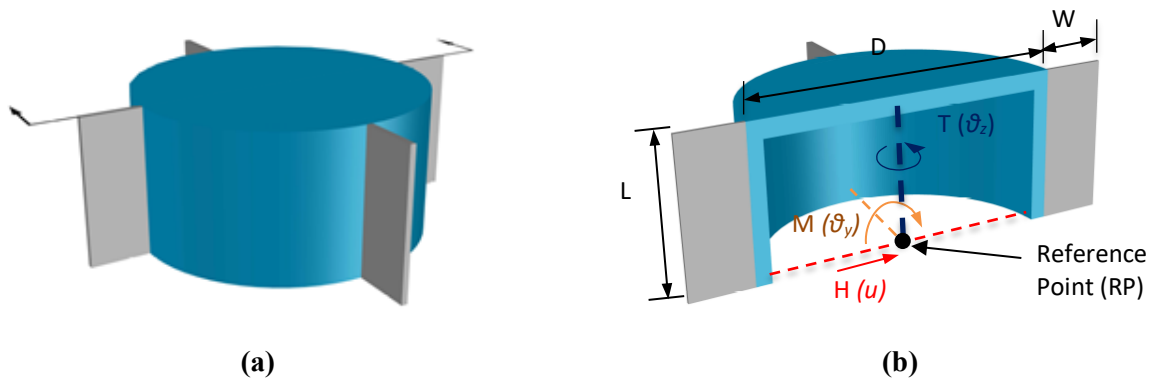


Figure 1. Winged Suction Caisson, $L/D=0.5$, $W/D=20\%$

A particular focus of this research is to determine torsional capacity of the proposed winged caissons in undrained conditions using finite element analysis. Three-dimensional finite element models of the winged caissons and the foundation will be produced with PLAXIS 3D and the capacity of the new SCF will be investigated under both uniaxial and combined horizontal, moment and torsional loadings. The results will be presented as a series of failure envelopes for various wing sizes and embedment depths.

METHODOLOGY

Geometry and Material Parameters

Embedment to diameter ratios (L/D) of 0 (surface foundation), 0.25, 0.5, 0.75 and 1 were modelled, where L is the skirt length and D is the diameter of the caisson. The SCF was modelled with a diameter of 12m for each of the analyses to replicate the prototype foundation installed in Frederikshavn, Denmark (Houlsby et al, 2005). A surface foundation was modelled solely to determine the uniaxial capacity of the foundation. In addition, wing widths (W) of 0% (no wings), 10%, 20% and 30% of the caisson diameter were adopted. The winged SCF was orientated so that two of the wings were perpendicular to the direction of loading.

Similar to Taiebat and Carter (2005) and Hung and Kim (2014), the soil was modelled as a soft clay of extremely low strength, which is representative of the ground conditions encountered in the North Sea and The Gulf of Mexico (*De Ruiter and Fox, 1976; Jeanjean et al, 1998*). The soft clay was modelled as perfectly elastic-plastic based on the Tresca failure criterion with an effective unit weight (γ') of 6 kN/m³, a Poisson's ratio (ν) of 0.495 and a uniform undrained shear strength (s_u) of 5 kN/m². These typical parameters have been derived from correlations provide in BS8002 (*BSI, 2015*), BS EN ISO 14688-2 (*BSI, 2018*) and Carter and Bentley (1991). An undrained Young's modulus to undrained shear strength ratio of 300 was assigned to the homogenous clay soil as proposed by Bowles (1997).

The Tresca yield criterion was adopted as it is applicable for clay soils deforming under undrained loading, meaning the elastic and plastic components of the volumetric strain are equal to zero. The main advantage of using this elastic-plastic model is that there are a small number of input parameters (Schweiger, 2008). The soil was modelled using 10-noded tetrahedral elements. The soil and caisson interface was modelled as fully bonded (i.e. fully rough in shear with no separation) as tension cracks are unlikely to occur in soft clay under undrained loading unless large displacements occur (*Vulpe et al, 2014; Gourvenec, 2008*).

As the stiffness of the SCF is much greater than that of the surrounding soil, the caisson has been modelled as a rigid body. This prevents individual constituent elements deforming but allows a single reference point (RP) to be defined about which the body can translate or rotate (*Gourvenec, 2008; Plaxis, 2017*). The RP was assigned to the base of the foundation as suggested in previous studies to maintain a positive moment when a horizontal load is applied about the base of the foundation (*Butterfield et al, 1997; Gourvenec, 2008; Hung and Kim, 2014*). The RP and standardised sign convention adopted in this study are illustrated in Fig. 1b.

Mesh

The finite element mesh constructed for an L/D of 1 is presented in Fig. 2(a). A similar mesh discretisation was adopted for each of the analyses for different embedment depths and wing widths. The mesh is locally refined at the location of the caisson wall/soil interface where the largest deformations and stresses will occur, as illustrated in Fig. 2(b) (*Mehravar et al, 2016*). Numerous mesh densities and domains were initially considered and were refined locally until the results converged. This mesh convergence study enabled an accurate solution to be obtained within a reasonable computation time. It was concluded that a finite element (FE) domain of $12D \times 12D \times 4L$ would be adopted so as not to affect the response of the foundation. Displacements at the base of the mesh were fixed in all orientations and the vertical boundaries were restrained laterally.

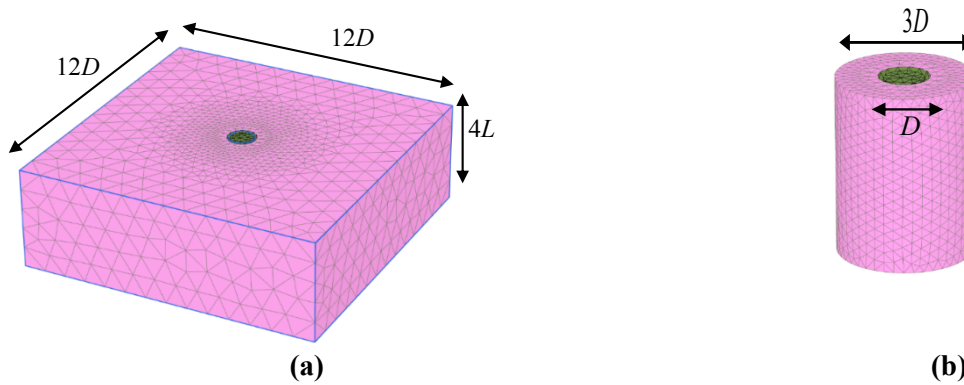


Figure 2. Winged caisson half model notation and sign convention

Loading path

Each numerical analysis was displacement controlled, where the horizontal (u), moment (θ_y) and/or torsional (θ_z) displacements were applied at the RP. This method allows post-failure conditions to be predicted and therefore is more suitable for predicting the failure load than the stress-controlled method (*Bransby and Randolph, 1998; Mehravar et al, 2016*).

The ultimate capacity of the foundation under combined loading is presented graphically as a series of failure envelopes. The boundary of the envelope represents yielding of the foundation with associated plastic hardening (*Mehravar et al, 2016; Bransby and Yun, 2009*). The extremities of the failure envelope were

established by undertaking a series of uniaxial analyses to determine the ultimate horizontal (H_{ult}), moment (M_{ult}) and torsional (T_{ult}) capacity under pure loading (e.g. H_{ult} : $V, M, T = 0$). The yield point is assumed to correspond to the ultimate capacity and was established using the tangent intersection method proposed by Mansur and Kaufman (1958). This comprises drawing two tangential lines, one along the initial section of the load-displacement curve and the other along the later section. The point at which the two lines intersect gives the bearing capacity (Hung and Kim, 2014).

To create a failure envelope under combined loading, both the ‘swipe’ and the fixed ratio displacement ‘probe’ method were initially employed. The probe method comprises applying a fixed ratio of displacement (e.g. $\Delta\theta_z/\Delta u$) to the SCF. The load path starts at the origin and the gradient initially follows an elastic response. The displacement is increased until the foundation loading converges at a specific point on the yield surface. Subsequent points on the yield surface were established by varying the fixed displacement ratio (Bransby and Randolph, 1998).

The swipe method involves prescribing a displacement or rotation to one degree of freedom until the ultimate capacity is achieved. The second phase (swipe) entails applying a displacement or rotation to another degree of freedom whilst keeping the displacement or rotation increment from the first phase equal to zero. The swipe phase closely tracks the true failure envelope as minor expansion of the yield surface is required to balance the small elastic deformation (Bransby and Randolph, 1998). Supachawarote, et al, (2005) found that the swipe method significantly underestimates the true failure envelope where foundations are embedded. However, the swipe method has been widely adopted due to its simplicity and the fact that most of the yield surface can be established from a single test (Gourvenec, 2008). Therefore, in this study a sensitivity analysis has been undertaken to identify the most suitable method for determining the shape and size of the failure envelope for winged SCFs under combined loading.

Validation of the numerical modelling

The reliability of the finite element model was validated by comparing the results with those of Taiebat and Carter (2005) and Suroor and Hossain (2015) who considered uniaxial and combined horizontal and torsional loading on a suction caisson/pile foundation with an embedment length to diameter ratio of 2. The ultimate uniaxial torsional capacity predicted by the finite element analysis in this study was $3.6s_u D^3$ compared to a value of $3.4s_u D^3$ and $3.52 s_u D^3$ predicted by Taiebat and Carter (2005) and Suroor and Hossain (2015) respectively. This yields a percentage difference of between 2% and 6% which is within tolerable limits for a finite element analysis.

In addition, the combined horizontal and torsional loading failure envelope was derived using the probe method and is compared to that of Taiebat and Carter (2005) in Fig. 3. The failure envelope derived from the numerical model used in this study appears to be in close agreement with that of Taiebat and Carter (2005). Thus, it was concluded that the soil/caisson interface could be reasonably simulated using the finite element model. The validated model was subsequently extended to predict the behaviour of a SCF subjected to uniaxial and combined horizontal, moment and torsional loading for a range of embedment to diameter ratios and wing widths.

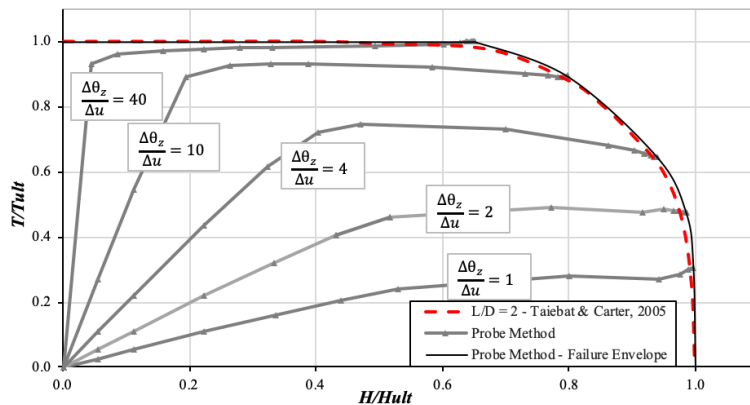


Figure 3. Validation of numerical model using failure envelope in the H-T normalised load space

RESULTS AND DISCUSSIONS

Uniaxial loading

Fig. 4 presents the ultimate horizontal capacity as a bearing capacity factor ($N_c H_{ult} = H_{ult} / A \cdot s_u$) expressed as a function of embedment depth and wing width.

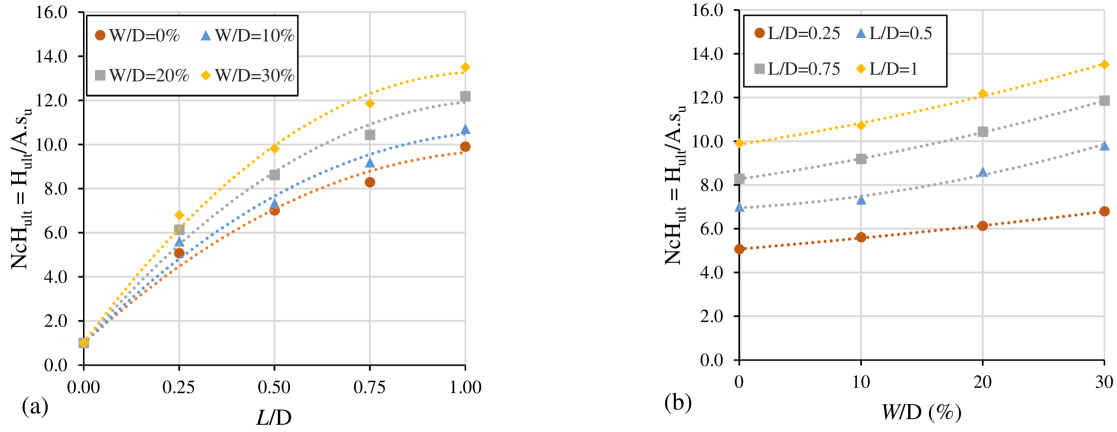


Figure 4. Ultimate horizontal capacity (bearing capacity factor)

Fig. 4(a) shows that a winged SCF can mobilise the same ultimate horizontal capacity as a conventional SCF at a reduced embedment depth. The ultimate horizontal capacity for both conventional (i.e. without wings) and winged SCFs increases with embedment depth at a decreasing rate. This is due to coupling between the horizontal and rotational degrees of freedom, as reported by Gourvenec (2008). The coupling effect is more pronounced for $L/D \geq 0.5$ as the failure mechanism is governed more by rotation than sliding with increased embedment depth, as shown in Fig. 5. The centre of rotation of the SCF increases in depth below ground level with increasing embedment.

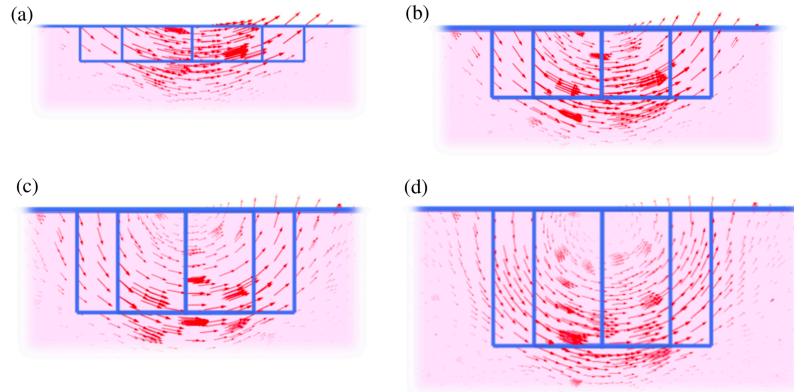


Figure 5. Failure mechanism under horizontal loading (H_{ult}) ($W/D=30\%$) (a) $L/D=0.25$ (b) $L/D=0.5$ (c) $L/D=0.75$ (d) $L/D=1$

Fig. 4(b) shows that the ultimate horizontal capacity of a SCF increases with wing width. The ultimate horizontal capacity for an L/D of 1 increases by 8%, 23% and 36% for W/D ratios of 10%, 20% and 30% respectively, in comparison to a conventional SCF. The winged SCF increases the volume of soil sheared and the lateral extent of the failure mechanism, as illustrated in Fig. 6. A larger amount of passive resistance is mobilised within the soil, increasing the horizontal capacity of the foundation.

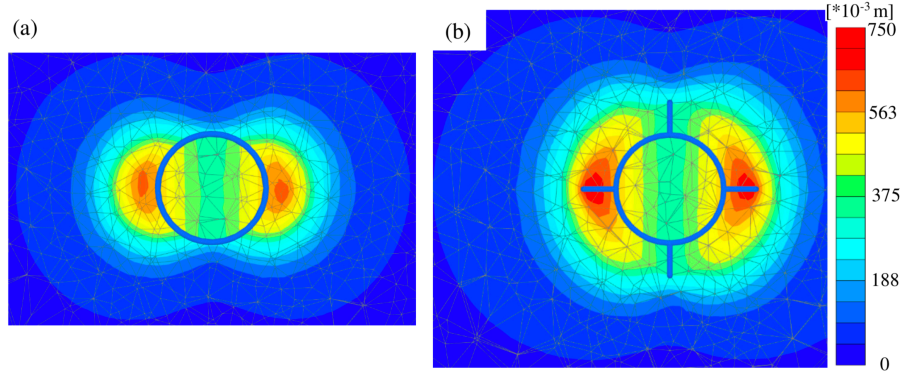


Figure 6. Total displacement under horizontal loading – plan view ($L/D=1$) (a) $W/D=0\%$ (b) $W/D=30\%$

The ultimate horizontal capacity of a winged SCF is provided by a combination of the normal passive resistance, radial shear and base shear resistance, as illustrated in Fig. 7. The bearing capacity factors presented in Fig. 4 can be expressed as a depth factor where $d_c H_{ult} = N_c H_{ult(L/D)} / N_c H_{ult(L/D=0)}$. This is shown graphically in Fig. 8. Additionally, the ultimate horizontal capacity can be expressed using Equation 1 which considers both embedment depth and wing width.

$$d_c H_{ult} = 1 + a_1 \left(\frac{L}{D} \right) + a_2 \left(\frac{L}{D} \right)^2 \quad (1)$$

where

$$a_1 = 15.12 + 0.27 \left(\frac{W}{D} \right) \quad (2)$$

$$a_2 = -6.9937 - 0.0364 \left(\frac{W}{D} \right) - 0.0035 \left(\frac{W}{D} \right)^2 \quad (3)$$

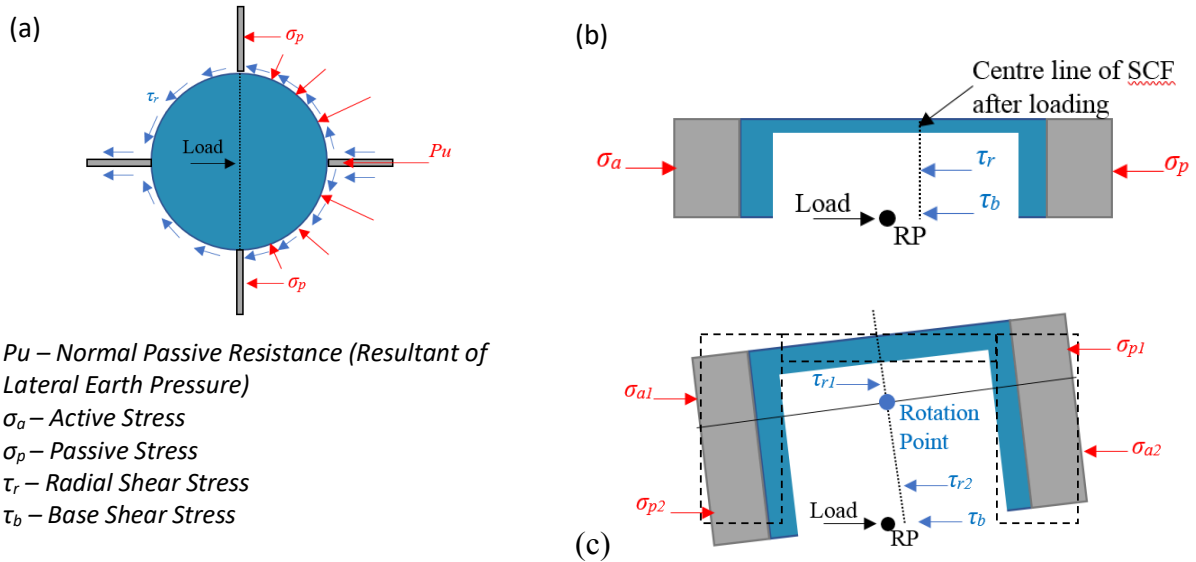


Figure 7. Distribution of stresses along winged SCF (a) Plan View (b) $L/D < 0.5$ (c) $L/D \geq 0.5$

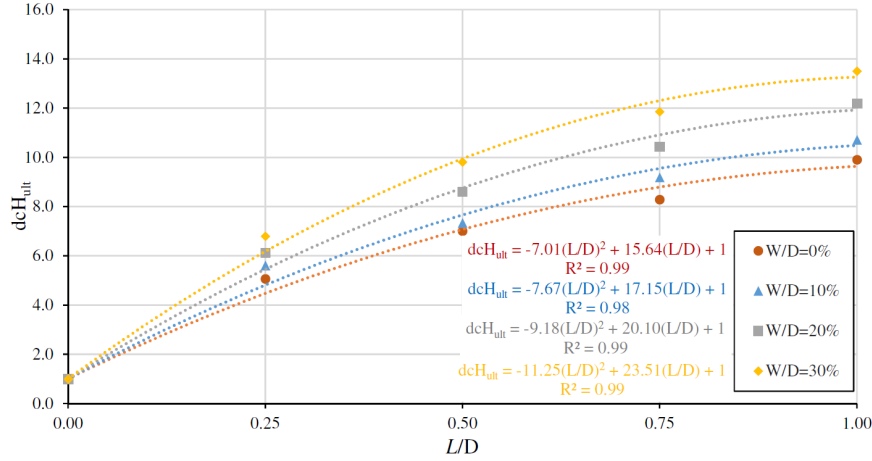


Figure 8. Ultimate horizontal capacity depth factor as a function of L/D and W/D ratios

In a similar fashion to horizontal capacity, the ultimate moment capacity can be expressed using a quadratic equation which include both embedment depth and wing width (Equation 4). It is worth mentioning that the addition of wings to a SCF with an L/D of 1 increases the ultimate moment capacity by 9%, 26% and 43% for W/D ratios of 10%, 20% and 30%. The ultimate moment capacity of the foundation is dependent on the earth pressure distribution along the caisson wall (Zhang *et al*, 2016) and as previously stated the inclusion of wings provides additional passive soil resistance.

$$d_c M_{ult} = 1 + b_1 \left(\frac{L}{D} \right) + b_2 \left(\frac{L}{D} \right)^2 \quad (4)$$

where

$$b_1 = 0.1784 - 0.0055 \left(\frac{W}{D} \right) + 0.0014 \left(\frac{W}{D} \right)^2 \quad (5)$$

$$b_2 = 2.5406 + 0.0371 \left(\frac{W}{D} \right) - 0.0007 \left(\frac{W}{D} \right)^2 \quad (6)$$

Ultimate torsional capacity

Fig. 9 presents the ultimate torsional bearing capacity factor ($N_c T_{ult} = T_{ult} / A.D.s_u$) as a function of embedment ratio and wing width. The ultimate torsional capacity of the SCF increases non-linearly with both increasing embedment depth and wing width.

The ultimate torsional capacity of a conventional SCF increases by approximately 58%, 100% and 139% for L/D of 0.5, 0.75 and 1 respectively, relative to a L/D of 0.25. The torsional capacity of the caisson increases with increasing embedment depth due to the caisson having a greater surface area in contact with the soil resulting in greater frictional resistance being mobilised. The rotational failure mechanism induced is presented in Fig. 10. Frictional resistance is shown to be mobilised on both the inner and outer sections of the caisson. The soil within the caisson is likely to have experienced large strains during installation and therefore a reduced frictional resistance will be mobilised. However, the disturbance effects caused by the installation of the SCF are outside of the scope of this study and will not be considered further.

Fig. 9(b) shows that the ultimate torsional capacity for an L/D of 1 increases by 146%, 251% and 343% with the inclusion of wings with a W/D ratio of 10%, 20% and 30% respectively. The substantial improvement in the torsional capacity with increasing wing width can be explained by the additional passive resistance mobilised in the soil behind the wings and the increased volume of soil sheared, as shown in Fig. 10(b). This failure mechanism shows that the largest displacements occur at the location of the wings and adjacent to the caisson skirt. The stresses mobilised in the soil are presented diagrammatically in Fig. 10(c).

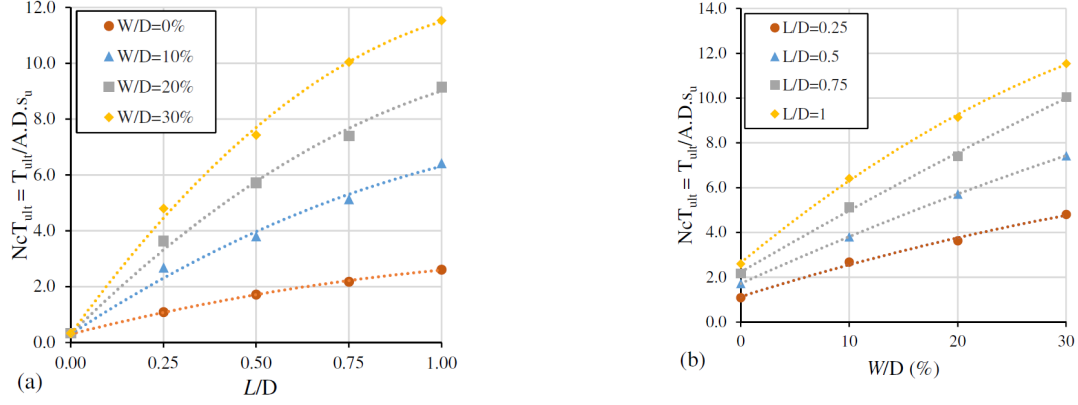


Figure 9. Ultimate torsional capacity (bearing capacity factor)

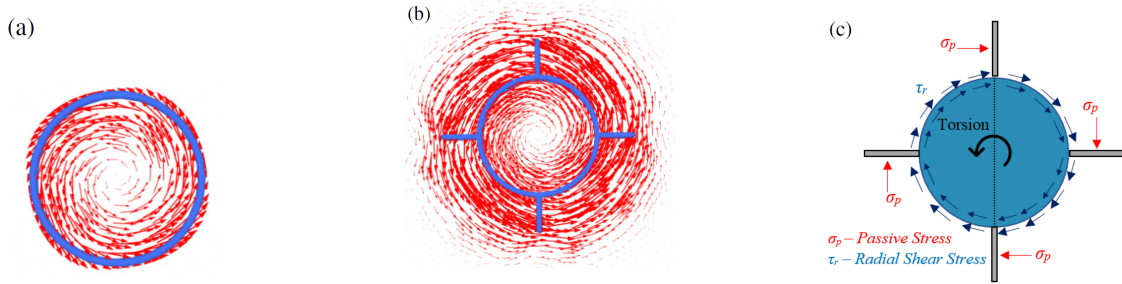


Figure 10. Ultimate torsional loading (a) Failure Mechanism $L/D=1$, no wings (b) Failure Mechanism $L/D=1$, 30% wings (c) Distribution of Stresses along winged SCF

The bearing capacity factors presented in Fig. 9 can be expressed as a depth factor where $d_c T_{ult} = N_c T_{ult(L/D)} / N_c T_{ult(L/D=0)}$. The ultimate torsional capacity can be expressed using the following quadratic equation which considers both embedment depth and wing width.

The ultimate torsional capacity can be expressed using the following quadratic equation which considers both embedment ratio and wing width.

$$d_c T_{ult} = 1 + c_1 \left(\frac{L}{D} \right) + c_2 \left(\frac{L}{D} \right)^2 \quad (7)$$

where

$$c_1 = 9.9963 + 1.4889 \left(\frac{W}{D} \right) \quad (8)$$

$$c_2 = -2.1699 - 0.6068 \left(\frac{W}{D} \right) \quad (9)$$

From the uniaxial analyses it can be concluded that adding wings to the SCF can considerably increase the ultimate torsional capacity of the foundation, whilst having the secondary benefit of improving both the horizontal and moment capacity.

COMBINED LOADING

Comparison of swipe and probe method

This section assesses the suitability of the swipe and probe method in deriving the failure envelope under combined horizontal and torsional loading for a winged SCF with a L/D of 1 and W/D of 10%. The failure envelope in H-T normalised load space is presented in Fig. 11.

Whilst the probe method was used successfully in the validation of the numerical model presented in this study, it is more difficult to implement for winged SCFs. Fig. 11 illustrates that for each ratio of combined displacement there is no distinct point at which the loads ‘converge’. This was observed for each of the wing

widths modelled. An assumed failure surface, based on the individual load-displacement curves, is provided in Fig. 11 for illustrative purposes.

Similar to Supachawarote et al (2008), the swipe method (H,T) was found to underestimate the torsional load for a given horizontal load by up to 18%, in comparison to the assumed failure surface derived from the probe method. The degree of conservatism increases as the failure envelopes approaches the ultimate torsional capacity. This is because zones of plasticity occur within the soil prior to bearing failure resulting in the swipe method tracking a load path inside the true failure envelope (Bransby and Randolph, 1998). In addition, it was also found that the swipe method is sensitive to the initial direction of displacement/rotation. The two applications of the swipe method presented in Fig. 11 (H, T & T, H) result in a different sequence of failure mechanisms occurring and hence produce two different failure envelopes. Nouri et al (2012) state that the swipe method should be initially displaced in the degree of freedom under examination. In this study the effect of torsional loading on the horizontal and moment capacity is considered, meaning that the initial displacement will be in the horizontal and moment degrees of freedom.

Although the swipe method underestimates the size of the failure envelope, it is a more robust repeatable technique than the probe method and has been widely adopted by Bransby and Randolph (1998), Gourvenec (2008) and Mehravar et al (2016). Hence the swipe method will be utilised in this study to evaluate the effect that adding wings has on the capacity of the SCF.

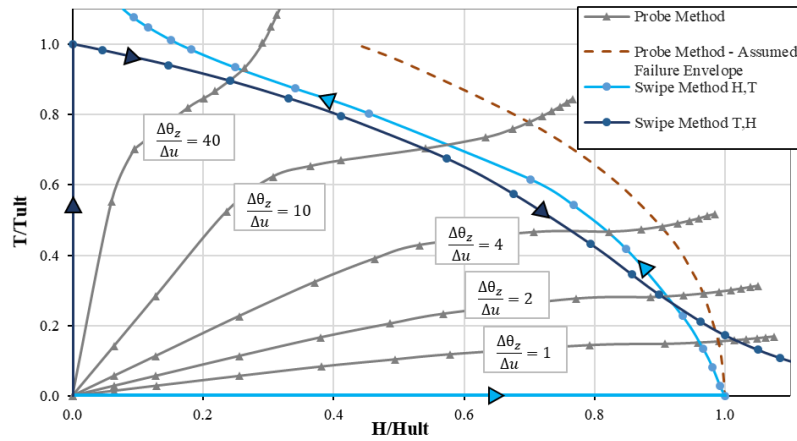


Figure 11. Comparison of failure envelopes predicted using the swipe and probe method in H-T normalised load space.

Combined Torsion and Moment Capacity

The failure envelopes under combined moment and torsional loading in dimensionless load space ($M/A.D.s_u$, $T/A.D.s_u$) are provided in Fig. 12. The size of the failure envelope increases with both wing width and embedment depth. For a given dimensionless moment load of $4A.D.s_u$ the torsional capacity of the SCF with an L/D of 1 increases by 73%, 184% and 300% for wing widths of 10%, 20% and 30% respectively. This again illustrates the improvement in the overall capacity of the SCF with increased wing width. The results shown in Fig. 12 are representative of the trends experienced for each of the embedment ratios and wing widths modelled.

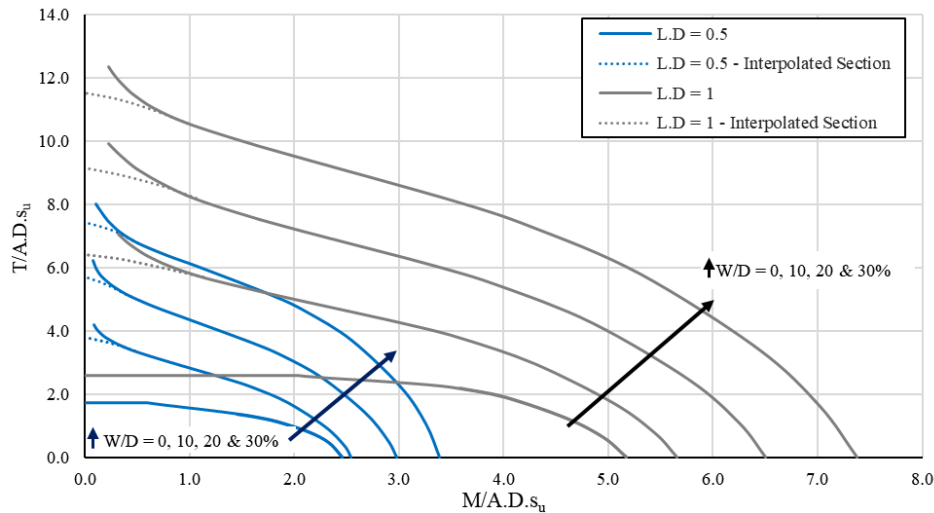


Figure 12. Effect of wing width on the size of the failure envelope in M-T dimensionless load space for L/D of 0.5 and 1 and $0\% \leq W/D \leq 30\%$

CONCLUSIONS

This study has investigated the torsional capacity of winged SCFs subjected to horizontal loads and overturning moments in soft, extremely low strength clay soil using a 3D FE model. With the addition of four wings to the SCF, the ultimate torsional capacity is increased by between 146% and 343% depending on wing width for an L/D of 1 compared to a conventional SCF. There is also the secondary benefit that both the ultimate horizontal and moment capacity are increased by up to 44% with the addition of wings.

A comparison between ‘swipe’ and ‘probe’ methods to determine the failure envelope for combined loading was conducted. Under combined loading the size of the failure envelope in M-T dimensionless load space increase with both wing width and embedment depth. The enhancement in capacity is due to the additional volume of soil sheared at the location of the wings, thus providing increased passive resistance. Hence the addition of wings makes the SCF a more attractive proposition for use as the foundation for offshore wind turbines in comparison to the more expensive, less sustainable monopile foundation.

Further studies should assess the behaviour of a winged SCF within normally consolidated soils with an increasing strength profile with depth. This is likely to have an influence on the embedment depth of the SCF. In addition, various wing profiles should be considered to optimise the shape of the wings yielding a more economically viable solution. Furthermore, potential additional installation challenges should be thoroughly analysed to ensure the suitability of the wings for SCFs.

REFERENCES

- Bienen, B., Gaudin, C., Cassidy, M. J., Rausch, L., Purwana, O. A., and Krisdani, H. (2012) ‘Numerical modelling of a hybrid skirted foundation under combined loading’, *Computers and Geotechnics*, 45, pp. 127–139.
- Bowles, J. E. (1997) *Foundation Analysis and Design*. 5th edn. Singapore: McGraw-Hill
- Bransby, M. F. and Randolph, M. F. (1998) ‘Combined loading of skirted foundations’, *Géotechnique*, 48 (5), pp. 63–65.
- Bransby, M. F. and Yun, G. (2009) ‘The undrained capacity of skirted strip foundations under combined loading’, *Géotechnique*, 59 (2), pp. 115–125. doi: 10.1680/geot.2007.00098.
- British Standards Institution (2015) BS8002: Code of Practice for Earth Retaining Structures. Available at: <https://shop.bsigroup.com/> (Accessed: 5 September 2018).
- British Standards Institution (2018) BS EN ISO 14688-2: Geotechnical Investigation and Testing – Identification and Classification of Soil. Available at: <https://shop.bsigroup.com/> (Accessed: 5 September 2018).
- Butterfield, R., Houlsby, G. T., and Gottardi, G. (1997) ‘Standardised sign conventions and notation for generally loaded foundations’, *Géotechnique*, 47 (5), pp. 1051–1054.
- Byrne, B. W. (2000) ‘Investigations of suction caissons in dense sand’, DPhil thesis, University of Oxford.
- Byrne, B. W., Houlsby, G. T., Martin, C. M., and Fish, P. (2002) ‘Suction caisson foundations for offshore wind turbines’ *Wind Engineering*, 26 (3), pp. 145–155.
- Carrington, D. P. (2013) ‘Suction bucket’ lays new foundation for offshore wind, *The Guardian*, 22 January. Available at: <https://www.theguardian.com/environment/2013/jan/22/suction-bucket-offshore-wind> (20 February 2018).
- Carter, M. and Bentley, S. P. (1991) *Correlations of Soil Properties*, London: Pentech Press.

- De Ruiter, J. and Fox, D. A. (1976) 'Site Investigations for the North Sea Forties Field', *Ground Engineering*, pp 25-30.
- Department of Energy (2016) *Wind Vision: A new era for wind power in the United States*. Available at: <https://www.energy.gov/eere/wind/maps/wind-vision> (Accessed: 12 March 2018).
- Emanuel, K. (2005) 'Increasing destructiveness of tropical cyclones over the past 30 years', *Nature*, 436 (7051), pp. 686–688. doi: 10.1038/nature03906.
- Gourvenec, S. (2008) 'Effect of embedment on the undrained capacity of shallow foundations under general loading', *Géotechnique*, 58 (3), pp. 177–185. doi: 10.1680/geot.2008.58.3.177.
- Houlsby, G. T., Ibsen, L. B., and Byrne, B. W. (2005) 'Suction caissons for wind turbines', *Proceedings of the international symposium on frontiers in offshore geotechnics*, pp. 75-94. London: Taylor and Francis.
- Hung, L. C. and Kim, S. R. (2014) 'Evaluation of undrained bearing capacities of bucket foundations under combined loads', *Marine Georesources & Geotechnology*, 32 (1), pp. 76–92. doi: 10.1080/1064119X.2012.735346.
- Jeanjean, P., Anderson, K. H., Kalsnes, B. (1998) 'Soil Parameters for Design of Suction Caissons for Gulf of Mexico Deepwater Clays', *Offshore Technology Conference*. Houston, Texas, 4-7 May. doi:10.4043/8830-MS
- Kim, D., Choo, Y. W., Park, J. H., and Kwak, K. (2016) 'Review of offshore monopile design for wind turbine towers', *Japanese Geotechnical Society Special Publication*, 4 (7), pp. 158–162
- Knudsen, B. S. and Østergaard, M. U. (2013) 'Deformation and Bearing Capacity of Bucket Foundations in Sand', *Master of Science thesis*, Aalborg University
- Li, D., Zhang, Y., Feng, L. and Gao, Y. (2015) 'Capacity of modified suction caissons in marine sand under static horizontal loading', *Ocean Engineering*, 102, pp. 1–16
- Mansur, C. I. and Kaufman, R. I. (1958) 'Pile tests, low-sill structure, Old River, Louisiana', *Transactions of the American Society of Engineers*, 123, pp. 715–743
- Mawer, B. and Kalumba, D. (2016) 'Stability of wind turbine foundations – accounting for gapping and eccentric loading', *Civil Engineering: Magazine of the South African Institution of Civil Engineering*, pp. 63–67
- Mehravari, M., Harireche, O., and Faramarzi, A. (2016) 'Evaluation of undrained failure envelopes of caisson foundations under combined loading', *Applied Ocean Research*, 59, pp. 129-137. doi: 10.1016/j.apor.2016.05.001.
- Nouri, H., Biscontin, G., and Aubeny, C. P. (2014) 'Undrained Sliding Resistance of Shallow Foundations Subject to Torsion', *Journal of Geotechnical and Geoenvironmental Engineering*, 140 (8), pp. 04014042-1–13. doi: 10.1061/(ASCE)GT.1943-5606.0001138.
- Plaxis (2017) *Plaxis 3D 2017 Reference Manual*.
- Schweiger, H. F. (2008) 'The role of advanced constitutive models in geotechnical engineering', *Geomechanics and Tunneling*, 1 (5), pp. 336–344. doi: 10.1002/geot.200800033
- Supacharawote, C., Randolph, M. R., and Gourvenec, S. (2005) 'The effect of crack formation on the inclined pullout capacity of suction caissons', *Proceedings of 11th International Conference on Computer Methods and Advances in Geomechanics*, Turin, Italy, pp. 577–584.
- Suroor, H. and Hossain, J. (2015) 'Effect of torsion on suction piles for subsea and mooring applications', *Proceeding of the 3rd International Symposium on Frontiers in Offshore Geotechnics*, pp. 325–330. doi: 10.1201/b18442-31
- Taiebat, H.A. and Carter, J. P. (2005) 'A failure surface for caisson foundations in undrained soils', *Proceedings 1st international symposium frontiers in offshore geotechnics*, Perth, Australia. . 10.1201/NOE0415390637.ch25.
- Vulpe, C., Gourvenec, S., and Power, M. (2014) 'A generalised failure envelope for undrained capacity of circular shallow foundations under general loading', *Géotechnique Letters*, 4 (3), pp. 187-196. doi.org/10.1680/geolett.14.00010.
- Zhang, Y., Li, D. and Gao, Y. (2016) 'Earth pressures on modified suction caisson in saturated sand under monotonic lateral loading', *Journal of Renewable and Sustainable Energy*, 8 (1), 053312. doi: 10.1063/1.4966701